Chinese Chemical Letters 37 (2026) 111443

Contents lists available at ScienceDirect

Chinese Chemical Letters

journal homepage: www.elsevier.com/locate/cclet

Inherently chiral molecular barrels *via* directional cascade hooping

Hao Zhou[a,b], Xu-Dong Wang[a], Yu-Fei Ao[a,b], De-Xian Wang[a,b], Qi-Qiang Wang[a,b,*]

[a] *Beijing National Laboratory for Molecular Sciences, CAS Key Laboratory of Molecular Recognition and Function, Institute of Chemistry, Chinese Academy of Sciences, Beijing 100190, China*
[b] *University of Chinese Academy of Sciences, Beijing 100049, China*

ARTICLE INFO

Article history:
Received 30 March 2025
Revised 27 May 2025
Accepted 10 June 2025
Available online 11 June 2025

Keywords:
Inherent chirality
Molecular cage
Desymmetrization
Imine condensation
Conformation interconversion

ABSTRACT

A kind of inherently chiral molecular barrels were efficiently constructed by a directional cascade hooping strategy. This strategy involves the anchoring of three nonsymmetric connecting arms onto a cap-dissymmetric bis(tetraoxacalix[2]arene[2]triazine) cage core, followed by hooping *via* imine condensation and reduction to afford the target molecular barrels with well-defined connectivity. The precise and high-yielding synthesis stems from both the bidirectional $C_{triazine}$-N bond flipping dynamics and the reversible nature of imine formation. The molecular barrels comprise a bis(tetraoxacalix[2]arene[2]triazine) core encircled by a 72-membered loop, forming three fan-shaped cavities with inherent chirality and multiple endo-functionalized sites. The existence of multiple diastereoisomeric conformers due to the restricted $C_{triazine}$-N bond flipping by the constrained loop structure was revealed by variable-temperature NMR studies and DFT calculations.

© 2026 Published by Elsevier B.V. on behalf of Chinese Chemical Society and Institute of Materia Medica, Chinese Academy of Medical Sciences.

Structurally sophisticated organic cage compounds have garnered significant attention in recent decades due to their aesthetic appeal, customizable multiple binding sites, and unique cavity microenvironments, which have facilitated diverse applications across various fields [1–7]. The incorporation of chirality further broadens their structural diversity and imparts chirality-related functionalities, such as chiroptical properties, chiral recognition, separation, and catalysis [8–12]. Typically, chiral cages can be synthesized either from enantiopure precursors or through post-modification with chiral auxiliaries, utilizing conventional stereogenic elements like point, axial, planar, and helical chirality. Recently, inherent chirality has emerged as a new term of chiral motif [13–18]. Initially coined to describe calixarenes with a typical ABCD arene array pattern lacking conventional stereogenic elements [13], this concept has since been extended to other macrocyclic and acyclic concave skeletons [14–23]. Despite the intriguing structural characteristics and properties associated with this chiral motif, its integration into higher-order molecular architectures, such as cage compounds, remains largely unexplored [24,25].

Previously, we successfully synthesized a D_{3h}-symmetric, prism-like bis(tetraoxacalix[2]arene[2]triazine) cage featuring two phloroglucinol caps and three triazine arms, which form three V-shaped electron-deficient cavities [26]. Owing to its straightforward synthesis, ease of modification, and unique structural features, the cage has proven to be an excellent platform for investigating anion–π recognition and self-assembly [27,28], cooperative anion–π catalysis [29–32], and for fabricating sophisticated molecular architectures [24,33–35] and cage-based framework materials [36–38]. To create more enclosed cavities, we developed a bottom-up anchor-hoop strategy, introducing a loop around the cage core *via* threefold ring-closing metathesis reactions, which enabled the efficient construction of a sophisticated molecular barrel (Fig. 1a, i) [33]. More recently, through hierarchical desymmetrization of the parent D_{3h}-symmetric cage, we achieved a new type of cage inherent chirality (Fig. 1a, ii) [24]. This desymmetrization strategy involved synthesizing a C_{3v} cage precursor with two distinct phloroglucinol caps, followed by progressive substitutions on the three triazine arms using different nucleophiles to yield the desired C_1-symmetric inherently chiral cages.

Inspired by these advancements, we envisioned further incorporating inherent chirality into the construction of molecular barrel through a directional cascade hooping strategy (Fig. 1b). By anchoring three suitable nonsymmetric connecting arms onto the C_{3v} cage precursor, two possible sequential connection pathways theoretically exist in the subsequent hooping step due to the existence of bidirectional flipping of the arms through $C_{triazine}$–N bond rotation. In such way, a pair of racemic C_3-symmetric inherently chiral molecular barrels could be readily formed. This one-pot cascade hooping process would allow for the rapid and efficient fabrication of novel sophisticated inherently chiral molecular barrels without the necessity for incremental, stepwise substitutions.

* Corresponding author.
E-mail address: qiqiangw@iccas.ac.cn (Q.-Q. Wang).

https://doi.org/10.1016/j.cclet.2025.111443
1001-8417/© 2026 Published by Elsevier B.V. on behalf of Chinese Chemical Society and Institute of Materia Medica, Chinese Academy of Medical Sciences.

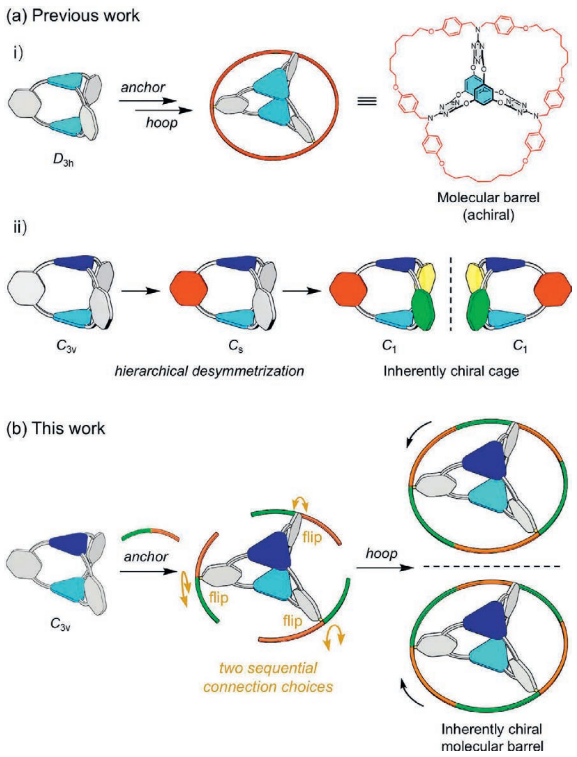


Fig. 1. (a) Previous work and (b) the conceptual design of inherently chiral molecular barrels through a directional cascade hooping strategy.

The synthesis route began by replacing the parent D_{3h}-symmetric cage with the previously reported tribromo-substituted C_{3v}-symmetric cage **1** [24], followed by the introduction of three non-symmetric amino anchoring arms (Scheme 1). To facilitate the subsequent directional cascade hooping process, the bifurcated arm **2**, featuring two distinct sides, a short side (in orange) and a long side (in green), was prepared (see Supporting information). The terminals of the sides can be readily converted to aromatic and alkyl amine sites for hooping connections, respectively. As anticipated, the nucleophilic substitution reaction of **1** with 3 equiv. of **2** afforded product **3** in a high yield of 93%. Under the conditions of $SnCl_2$ and HCl, deprotection of Boc groups and reduction of nitro groups occurred simultaneously, producing the hexa-amino cage product **4** in 89% yield.

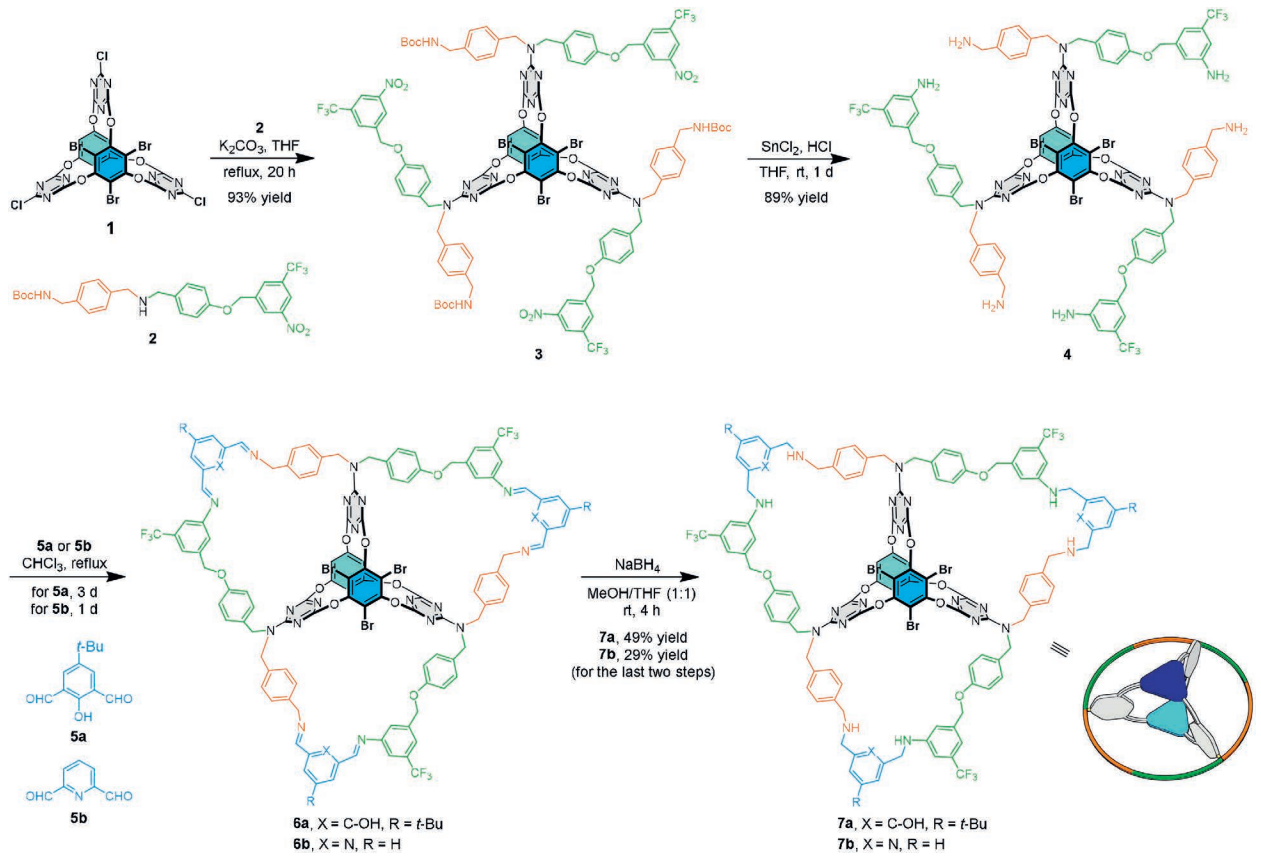
In the following hooping step, the dynamic imine condensation reaction [39–41] was employed. The thermodynamic control "error-correction" process would enable reversible connections between two adjacent terminal amine sites to favor the formation of the desired C_3-symmetric molecular barrels. Specifically, the inter-arm consecutive short side-long side connection could be promoted over other connection possibilities such as intra-arm connections, inter-arm short side-short side connections and long side-long side connections by geometry match (Fig. S8 in Supporting information). Such selectivity is necessary for the precise assembly of the target structure. In the initial attempt, the imine condensation reaction between **4** and three equivalents of *m*- or *p*-phthalaldehyde proved incomplete, yielding a complex mixture that included insoluble precipitates, but no desired product was detected. This result indicated that the appropriate reactivity and geometry of the aldehyde component must be considered.

Salicylic dialdehyde **5a** [42] was then selected for its enhanced solubility and reactivity attributed to intramolecular hydrogen bonding. The reaction of **4** with 3 equiv. of **5a** in $CDCl_3$ was *in-situ* monitored by ^{1}H NMR (Fig. 2a). Notably, the spectra revealed the gradual disappearance of the signals of the two reactants, accompanied by the emergence of two distinct sets of characteristic imine signals (δ 8.99, 8.59) and other relevant signals. The benzylic proton signals split into two sets of multiplets (δ 5.94–5.44, 4.11–3.94), indicative of the formation of an enclosed, restricted molecular barrel structure [33]. The reaction reached near completion after 3 days at room temperature. High-resolution mass spectrometry (HRMS) analysis of the reaction mixture displayed clear, predominant signals corresponding to the protonated species of the target molecular barrel **6a** (Fig. 2b and Fig. S4 in Supporting information).

Encouraged by these findings, a scaled-up reaction (0.25 mmol for **4a**) was conducted in $CHCl_3$ under reflux for 3 days to ensure full conversion (Scheme 1). The crude product was subsequently reduced using sodium borohydride, yielding the final molecular barrel **7a** in 49% yield (for two steps). This yield is notably high, considering the multiple reaction sites and many other connection possibilities. Given the efficient synthesis, 2,6-diformylpyridine **5b** was also subjected (Fig. S1 in Supporting information). Following imine condensation and reduction, a second molecular barrel product **7b** was obtained in 29% yield, demonstrating the adaptability of the cascade hooping strategy. Compared to other conventional macrocycle and cage construction approaches, this strategy highlighted the consecutive formation of six bonds at specific reaction sites to form a large, 72-membered macrocyclic loop encircling a cage core in a single step. The covalent templating effect exerted by the cage core and the inter-arm geometry match of the loop were crucial for the successful precise construction of the targeted molecular barrel structure.

The molecular barrels **7a** and **7b** were fully characterized by ^{1}H, ^{13}C NMR and HRMS (Fig. 3 and Figs. S2, S3, S5 and S6 in Supporting information). Taking **7a** as a representative example, ESI-MS analysis revealed exclusive signals for $[\mathbf{7a}+3H^+]^{3+}$ and $[\mathbf{7a}+2H^+]^{2+}$, corresponding to the protonated species of the target molecular barrel (Fig. 3a). The ^{1}H NMR spectrum exhibited a complex set of multiple signals at ambient temperature (Fig. 3b), consistent with observations in previously reported symmetric molecular barrel [33]. This complexity arises from the restricted flipping rotation of the three $C_{triazine}$–N bonds, which is caused by their partial conjugation with the electron-withdrawing triazine rings and being further constrained within the enclosed loop structure (Fig. 3c). The situation is further complicated in the newly synthesized inherently chiral molecular barrels due to the dissymmetric nature of both phloroglucinol caps and the entire loop. As a result, four pairs of diastereoisomeric conformers (each comprising a pair of enantiomers, donated as **A** and *ent*–**A**, for example) are theoretically possible. Among these, two conformers exhibit C_3-symmetry (**A** and **B**, with alternating up/down/up/down/up/down array or *vice versa*), while the other two are C_1-symmetric (**C** and **D**, with interrupted up/down/up/up/down/down array or *vice versa*). Due to the tightly enclosed loop structure, the interconversion between these diastereoisomers is slow on the NMR timescale at ambient temperature, thus resulting in complex NMR signals. However, upon increasing the temperature, the spectra simplified and eventually converged to a set of simple signals at 388 K (Fig. 3b), which corresponded to rapidly interconverted, averaged C_3-symmetric conformational characteristic. For **7b**, a similar interconversion process was also suggested by temperature-variable ^{1}H NMR spectra (Fig. S3 in Supporting information).

Since the dissymmetric arms are interconnected and locked within a loop structure, interconversion between the pair of enantiomers is impossible without deconstructing the molecular barrel structure, thereby preserving the inherent chirality stable. Numerous attempts were made to resolve the enantiomers using chiral high-performance liquid chromatography (HPLC) with different types of columns and various eluent systems, but remained unsuccessful (Table S1 in Supporting information). In addition, reso-



Scheme 1. Synthesis of inherently chiral molecular barrels. The drawing shows only one of the pair of enantiomers.

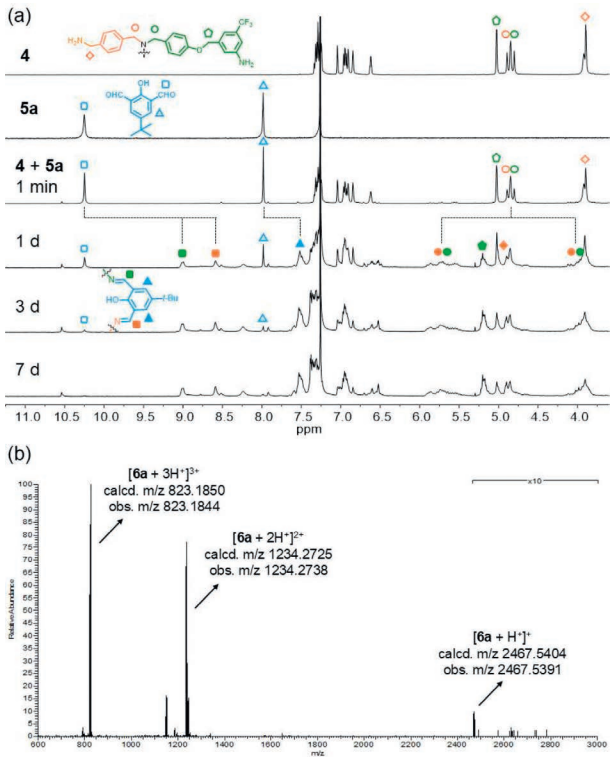


Fig. 2. (a) ^{1}H NMR monitoring (298 K, $CDCl_3$, 400 MHz) of the imine condensation reaction between **4** and **5a**. (b) High-resolution ESI-MS analysis of the reaction mixture of **4** and **5a** after 7 days.

lutions through co-crystallization with chiral acids (*e.g.*, camphorsulfonic acid, chiral phosphoric acid) or by derivation with chiral reagents like camphorsulfonyl chloride did not work out as well (see Supporting information for details). The resolution challenges likely stem from the molecular barrel's large, inward enclosed structure and the presence of intricate conformational isomerism.

To shed more light on the structure of the molecular barrels, DFT optimization was performed. Using **7a** as a representative example, the structures of all the four diastereoisomeric conformers were optimized (only one enantiomer was considered for each). As depicted in Fig. 4, the optimized structures reveal the expected "barrel" motif, featuring a bis(tetraoxacalix[2]arene[2]triazine) core encircled by a 72-membered loop (minimum atom connection) through three anchoring nitrogen sites. The two face-to-face phloroglucinol caps constitute top and bottom of the molecular barrel with a height of 4.5 Å (centroid-to-centroid distance). The molecular barrel bears three enclosed fan-shaped cavities separated by triazine rings with approximately 120° branching angles. The distances between the anchoring nitrogen atoms are around 11.5 Å. Since the two phloroglucinol caps are different and the loop is dissymmetric, each cavity is inherently chiral with an asymmetric ABCD pattern, rendering the whole molecular barrel chiral.

The four diastereoisomers differ in the orientation of their arms (1/3 loop segments) within the fan-shaped cavities (designated as "up" or "down" relative to the top Br-cap, Fig. 4). These varying orientations could have induced different degrees of twisting in the bis(tetraoxacalix[2]arene[2]triazine) moiety. Single-point energy calculations revealed that the C_1-symmetric conformers (**C** and **D**) are energetically more favorable than C_3-symmetric ones (**A** and **B**) (Table S2 in Supporting information). This was consistent with the observation in the crystal structure of the previously reported symmetric molecular barrel where a C_1-symmetric conforma-

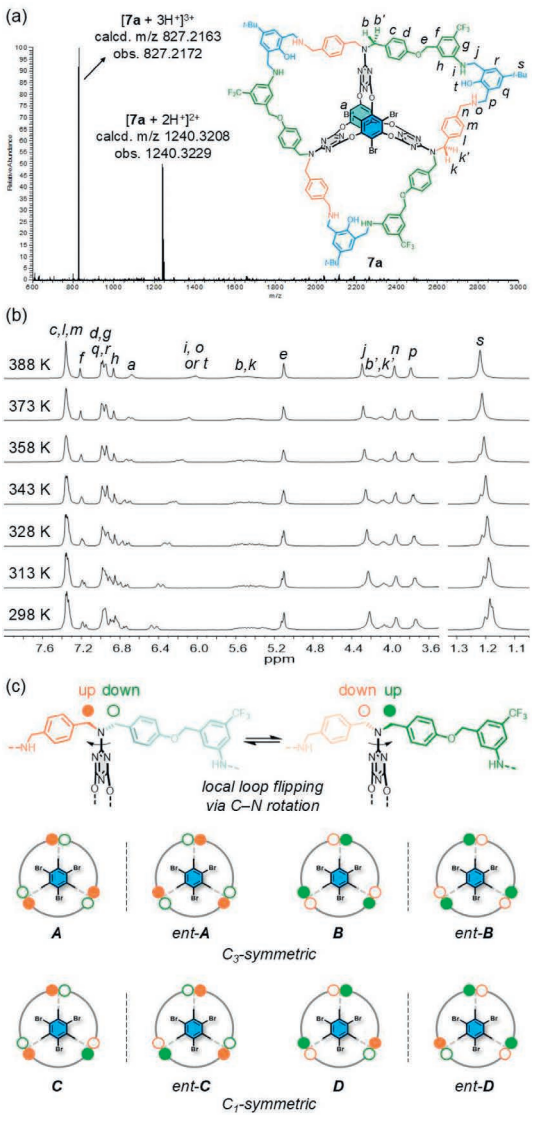


Fig. 3. (a) High-resolution ESI-MS of **7a**. (b) Temperature-variable ^{1}H NMR spectra (DMSO–d_6, 500 MHz) of **7a**. (c) Schematic representation for the possible conformational isomers of **7a** caused by the local loop flipping due to restricted $C_{triazine}$–N rotation.

tion existed [33]. This preference likely reflects a more relaxed loop configuration. While the C_3-symmetric form features three equivalent cavities, the C_1-symmetric conformers exhibit three distinct cavities with markedly different chiral microenvironments. Notably, in all optimized structures, both the amine N–H and phenolic O–H sites are oriented inward, creating a functionalized cavity environment. With the presence of fan-shaped electron-deficient π cavities and H-bonding sites on the loop, the molecular barrels could be a potential platform for investigating cooperative anion recognition. Moreover, the different conformers may open up opportunity for achieving dynamic, selective recognition by manipulating geometry-matched binding and synergistic conformational response. While preliminary titrations with methanesulfonate and camphor sulfonate anions did not show effective binding, further systematic investigation toward this direction is warranted.

In conclusion, we have successfully developed an efficient cascade hooping strategy to construct inherently chiral molecular barrels with precise structural control. This approach utilizes a cap-dissymmetric bis(tetraoxacalix[2]arene[2]triazine) cage precursor that directs the anchoring of three nonsymmetric con-

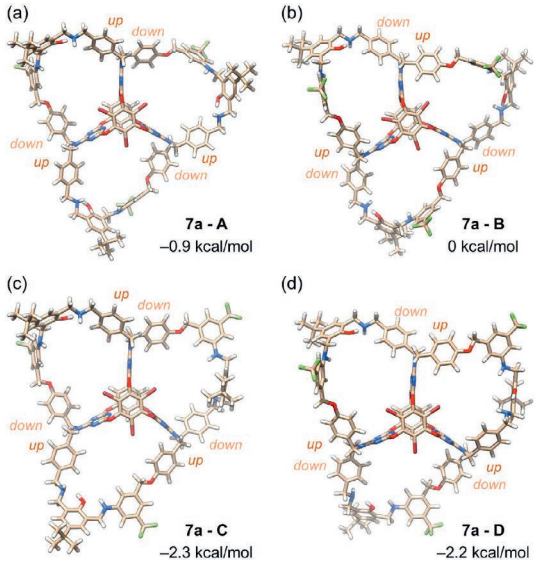


Fig. 4. DFT optimized structures (at M06–2X/6–31G(d) level) for the four conformational isomers of **7a**. The relative orientations of the arms in the fan-shaped cavities are designated as "up" or "down" with respect to the top Br-cap. The relative energy difference of the four conformers is shown (calculated at M06–2X/6–311G(d,p) level).

necting arms, followed by imine condensation and reduction to complete the loop structure. The synthesis benefits from both the bidirectional $C_{triazine}$-N bond flipping dynamics and the reversible nature of imine formation, enabling high-yielding formation of the target molecular barrels with well-defined connectivity. The molecular barrels feature a unique structure consisting of a bis(tetraoxacalix[2]arene[2]triazine) core surrounded by a 72-membered loop, creating three fan-shaped cavities with inherent chirality and multiple inwardly-directed functional groups. Variable-temperature NMR studies combined with DFT calculations revealed the existence of multiple diastereoisomeric conformers due to the restricted $C_{triazine}$-N bond flipping by the constrained loop structure. The one-pot cascade hooping strategy eliminates the necessity of incremental, stepwise connection, offering an efficient route for rapid construction of sophisticated inherently chiral architectures. This work extends the concept of inherent chirality to higher-order topological systems, opening new possibilities for novel chiral functional materials design, construction and exploring their diverse applications such as chiral recognition and supramolecular catalysis.

Declaration of competing interest

The authors declare that they have no known competing financial interests or personal relationships that could have appeared to influence the work reported in this paper.

CRediT authorship contribution statement

Hao Zhou: Methodology, Investigation, Formal analysis, Data curation. **Xu-Dong Wang:** Writing – review & editing. **Yu-Fei Ao:** Writing – review & editing. **De-Xian Wang:** Writing – review & editing. **Qi-Qiang Wang:** Writing – review & editing, Supervision, Project administration, Funding acquisition, Conceptualization.

Acknowledgment

Financial supports from National Natural Science Foundation of China (Nos. 21871276, 22022112, 21521002) are gratefully acknowledged.

Supplementary materials

Supplementary material associated with this article can be found, in the online version, at doi:10.1016/j.cclet.2025.111443.

References

[1] D.J. Cram, Nature 356 (1992) 29–36.
[2] H. An, J.S. Bradshaw, R.M. Izatt, Chem. Rev. 92 (1992) 543–572.
[3] L.R. MacGillivray, J.L. Atwood, Angew. Chem. Int. Ed. 38 (1999) 1018–1033.
[4] G. Zhang, M. Mastalerz, Chem. Soc. Rev. 43 (2014) 1934–1947.
[5] T. Hasell, A. Cooper, Nat. Rev. Mater. 1 (2016) 16053.
[6] G. Montà-González, F. Sancenón, R. Martínez-Máñez, V. Martí-Centelles, Chem. Rev. 122 (2022) 13636–13708.
[7] X. Yang, Z. Ullah, J.F. Stoddart, C.T. Yavuz, Chem. Rev. 123 (2023) 4602–4634.
[8] T. Brotin, L. Guy, A. Martinez, J.P. Dutasta, Enantiopure supramolecular cages: synthesis and chiral recognition properties, in: V. Schurig (Ed.), Differentiation of Enantiomers II, Topics in Current Chemistry, Differentiation of Enantiomers II, Topics in Current Chemistry, 341, Springer International Publishing, Switzerland, 2013, pp. 177–230.
[9] D. Zhang, A. Martinez, J.P. Dutasta, Chem. Rev. 117 (2017) 4900–4942.
[10] C. Li, Y. Zuo, Y.Q. Zhao, S. Zhang, Chem. Lett. 49 (2020) 1356–1366.
[11] X. Dong, H. Qu, A.C.H. Sue, X.C. Wang, X.Y. Cao, Acc. Chem. Res. 57 (2024) 1111–1122.
[12] L. Chen, M. Tan, J. Jin, et al., Chin. J. Org. Chem. 44 (2024) 2617–2639.
[13] V. Böhmer, D. Kraft, M. Tabatabai, J. Inclusion Phenom. Mol. Recognit. Chem. 19 (1994) 17–39.
[14] A.D. Cort, L. Mandolini, C. Pasquini, L. Schiaffino, New J. Chem. 28 (2004) 1198–1199.
[15] A. Szumna, Chem. Soc. Rev. 39 (2010) 4274–4285.
[16] G.E. Arnott, Chem. Eur. J. 24 (2018) 1744–1754.
[17] M. Tang, X. Yang, Eur. J. Org. Chem. 26 (2023) e202300738.
[18] W. Qin, G. Cera, Chem. Rec. 25 (2025) e202400237.
[19] B.Y. Hou, Q.Y. Zheng, D.X. Wang, M.X. Wang, Tetrahedron 63 (2007) 10801–10808.
[20] S. Guieu, E. Zaborova, Y. Blériot, et al., Angew. Chem. Int. Ed. 49 (2010) 2314–2318.
[21] J.W. Meisel, C.T. Hu, A.D. Hamilton, Org. Lett. 21 (2019) 7763–7767.
[22] S. Tong, J.T. Li, D.D. Liang, et al., J. Am. Chem. Soc. 142 (2020) 14432–14436.
[23] M.J. Gunther, X. Wang, J.D. Badjić, et al., Angew. Chem. Int. Ed. 60 (2021) 25075–25081.
[24] H. Zhou, Y.F. Ao, D.X. Wang, Q.Q. Wang, J. Am. Chem. Soc. 144 (2022) 16767–16772.
[25] S. Fang, Z. Bao, Z. Liu, et al., Angew. Chem. Int. Ed. 63 (2024) e202411889.
[26] D.X. Wang, Q.Q. Wang, Y. Han, et al., Chem. Eur. J. 16 (2010) 13053–13057.
[27] X.Y. Wang, J. Zhu, Q.Q. Wang, Y.F. Ao, D.X. Wang, Inorg. Chem. 58 (2019) 5980–5987.
[28] Z.Y. Li, C. Li, P. Li, et al., ChemPlusChem 85 (2020) 906–909.
[29] N. Luo, Y.F. Ao, D.X. Wang, et al., Angew. Chem. Int. Ed. 60 (2021) 20650–20655.
[30] N. Luo, Y.F. Ao, D.X. Wang, et al., Chem. Asian J. 16 (2021) 3599–3603.
[31] Q.Q. Wang, Acc. Chem. Res. 57 (2024) 3227–3240.
[32] M.S. Yue, N. Luo, X.D. Wang, et al., J. Am. Chem. Soc. 147 (2025) 2303–2308.
[33] Q.Q. Wang, N. Luo, X.D. Wang, et al., J. Am. Chem. Soc. 139 (2017) 635–638.
[34] C. Yu, Y. Yang, Y. Wang, New J. Chem. 45 (2021) 22049–22052.
[35] Q. Zhu, H. Qu, G. Avci, et al., Nat. Synth. 3 (2024) 825–834.
[36] J.X. Ma, J. Li, Y.F. Chen, et al., J. Am. Chem. Soc. 141 (2019) 3843–3848.
[37] B. Han, H. Wang, C. Wang, et al., J. Am. Chem. Soc. 141 (2019) 8737–8740.
[38] J. Wang, P. Yang, L. Liu, et al., CCS Chem. 4 (2022) 1879–1888.
[39] C.D. Meyer, C.S. Joiner, J.F. Stoddart, Chem. Soc. Rev. 36 (2007) 1705–1723.
[40] M. Mastalerz, Angew. Chem. Int. Ed. 49 (2010) 5042–5053.
[41] M.E. Belowich, J.F. Stoddart, Chem. Soc. Rev. 41 (2012) 2003–2024.
[42] M. Mastalerz, Chem. Commun. (2008) 4756–4758.